Kinematic coupling interchangeability

Anastasios John Hart*, Alexander Slocum, Patrick Willoughby

*Precision Engineering Research Group, Department of Mechanical Engineering, Massachusetts Institute of Technology,
77 Massachusetts Avenue, Room 3-470, Cambridge, MA 02139, USA*

Abstract

The deterministic nature of kinematic couplings enables closed-form characterization of interchangeability error, parametrized in terms of the magnitudes of manufacturing tolerances in the interface manufacturing and assembly processes. A process is suggested for calibrating kinematic couplings to reduce the interchangeability error, based on measurement of the contact points and calculation of a transformation matrix between the interface halves. A Monte Carlo analysis is developed and validated for predicting interchangeability of canoe ball kinematic couplings, and repeatability measurements and interchangeability simulation results are presented for kinematic coupling interfaces for the base and wrist of an industrial robot. Total mounting error, defined as the sum of the interchangeability and repeatability errors, appears to be dependent to first order only on the interface repeatability and the error of the interface calibration procedure.
© 2003 Elsevier Inc. All rights reserved.

Keywords: Kinematic coupling; Repeatability; Interchangeability; Modular; Error

1. Introduction

Traditional studies of kinematic couplings, such as those by Slocum and Donmez [1], Muller-Held [2], and Poovey et al. [3], have focused on the need for high interface repeatability; however, modular machines and instruments require rapid, accurate interchangeability. Interchangeability of a kinematic coupling is the tendency of the centroidal frame[1] of the top half of the interface to return to the same position and orientation relative to the centroidal frames of different fixed bottom halves when switched between them [4,5]. The centroidal frame is shown in Fig. 1, and interchangeability error is shown schematically by the mismatched centroidal frames in Fig. 2.

When a kinematic coupling is used to mount a machine or component, the mounting error arises from irregularities in the surface and preload conditions, manufacturing variation in the interface geometry, and environmental influences such as temperature changes. The translational and rotational components of these errors are reflected through the structural path of the machine by geometric transformations, giv-

ing the error contribution from the kinematic coupling at a point of measurement interest, such as the tool tip. The goal of this work is to model interchangeability and to determine if measurement of kinematic coupling contacts before interface mating can be used to decrease interchangeability error.

2. Kinematic coupling designs

A typical kinematic coupling mates a triangular configuration of three hemispheres on one interface plate to three "vee" grooves on another interface plate, thus enabling essentially exact constraint of the six degrees of freedom between the two bodies by Hertzian surface contact at six small regions. The main caveat to traditional ball–groove couplings, where the sphere diameters are approximately the widths of the vee grooves to which they mount, is that their kinematic nature means that their load capacity is limited to that of the small contact regions.

To achieve greater load capacity yet maintain repeatability, the "canoe ball" shape (named as such because it looks like the bottom of a canoe), evolved as shown in Fig. 3 to include an integrated tooling ball for calibration (discussed later). The "canoe" emulates the contact region of a ball as large as 1 m in diameter in an element as small as 25 mm across. However, a drawback of this design is the high cost of custom precision contour grinding the "ball" contact surfaces.

---

* Corresponding author. Tel.: +1-617-258-8541; fax: +1-617-258-6427.
 E-mail address: ajhart@mit.edu (A.J. Hart).
URL: http://pergatory.mit.edu.

[1] The centroidal frame has its origin at the centroid of the coupling triangle, *x*-axis aligned with the segment connecting the lower two balls, *y*-axis normal to the *x*-axis and in the plane defined by the three couplings (the coupling plane), and *z*-axis normal to the coupling plane.
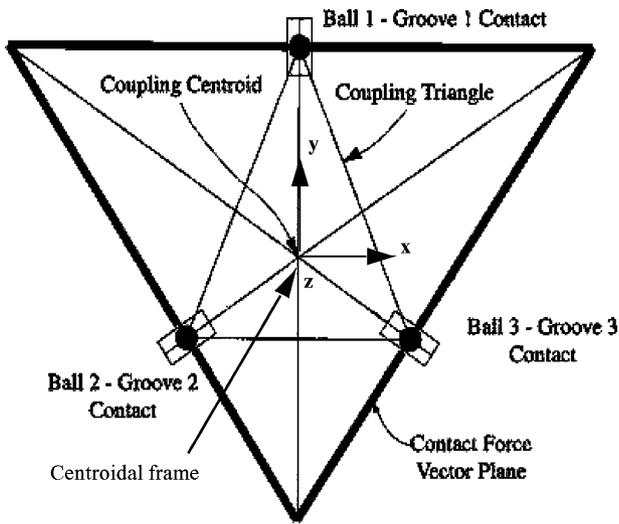
Fig. 1. Coupling triangle, showing coupling centroid and centroidal frame directions [5].

Fig. 3. Canoe ball coupling elements: (a) ball–groove assembly with tooling ball measurement feature; (b) exploded assembly.

As a cost-accuracy compromise, the three-pin quasi-kinematic coupling, shown in Figs. 4 and 5, was developed [4,6,7]. The three-pin coupling consists of an upper interface plate with a triangular arrangement of shouldered or dowel pins, coupled to a plate with a triangular arrangement of oversized cutouts with flat or curved contact surfaces with which the pins make contact. The pins are seated against the contact surfaces by i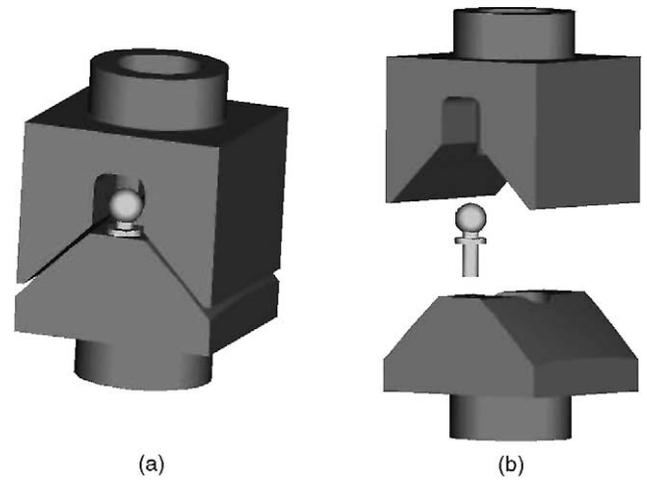ntroducing an in-plane preload force at the first pin using a bolt, compliant pin, or other mechanism. Flat contact surfaces, emphasized in Fig. 5, are simple to machine and ensure low contact stress for a given contact pin diameter. A three-pin coupling is designed by first defining the pin geometry and in-plane preload force to guarantee that the interface can be properly statically seated (overcoming friction), then defining the normal-to-plane preload needed to guarantee dynamic stability and give the desired stiffness.
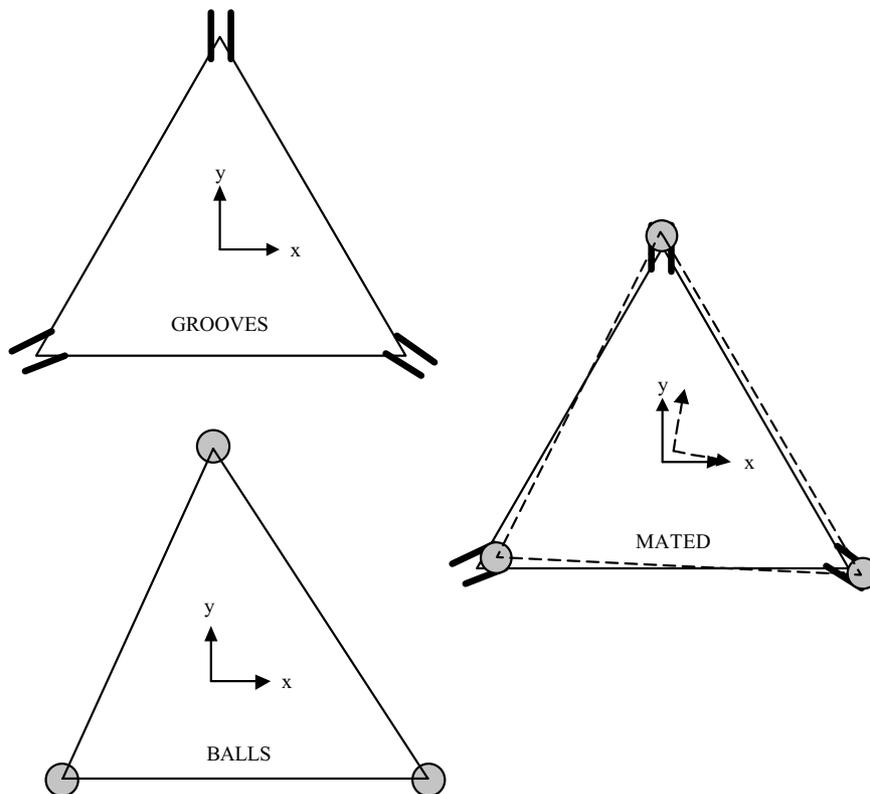

Fig. 2. In-plane error motion due to positional and angular perturbations of balls and grooves.
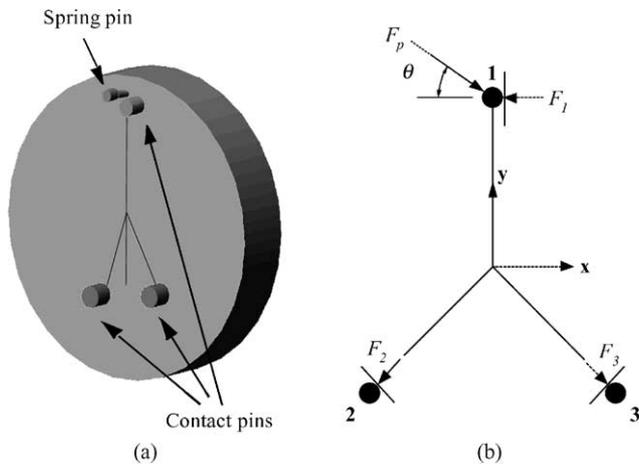
Fig. 4. Three-pin interface: (a) model of male half, with preload applied using a spring pin; (b) in-plane contact forces, with preload F_p and normal contact reactions F_1, F_2, and F_3.

3. Kinematic coupling interchangeability model

Neglecting the small variations in repeatability that may be caused by relatively larger errors in the coupling geometry, a first-order estimate of the total mounting error for a kinematic coupling is the sum of the repeatability and the interchangeability errors. Repeatability of heavily-loaded kinematic couplings is a well-studied effect, measured for typical ball–groove and canoe ball kinematic couplings to be on the order of 1 μm and better under well-controlled mounting conditions [1,2]. Friction is one of the biggest detriments to repeatability, and cannot be accounted for by calibration. Hale presents a quantitative method for estimating average frictional nonrepeatability as a function of ball and groove geometry and the coefficient of friction between the ball and groove [8]. Schouten et al. showed that incorporating flexures (e.g. by EDM) into groove surfaces can reduce friction sufficiently to increase coupling repeatability by a factor of 2 or more [9].

Interchangeability, on the other hand, is a deterministic geometric error. The kinematic behavior of a triangular layout reduces interchangeability error at the center of stiffness (the coupling centroid) to about one-third of the error of the coupling placements. The remaining error can be reduced by mapping the geometric errors based on the measured positions and orientations of each of the balls and grooves. This allows coupling elements to be measured, and the measured data to be incorporated in a model that determines a set of mapping coefficients for the interface.

Additional systematic errors arise from deflection of the coupling contacts and the interface plates due to applied disturbance forces and thermal expansion. Considering an interface that is designed with proper stiffness and thermal management considerations in mind, these errors are neglected by this model. Past research has demonstrated that the deflections due to Hertzian contact are not as significant as errors from geometric tolerances when couplings are manufactured using traditional machining and assembly processes [10,11].

3.1. Layout

To understand the effects of interchangeability error, first consider a general machine design application in which two modules mate through an interface of ball–groove kinematic couplings. Fig. 6 depicts a cell layout for an industrial robot with a kinematic coupling base mounting, where the grooves sit on a plate fixed to the floor and the mating balls are attached to the foot of the robot. Reference coordinate frames are placed centroidally on the groove set (A_{Groove}) and the ball set (A_{Ball}), and the couplings are secured using a sufficient (e.g. bolted) preload. For the work task, the tool center point (TCP) and co-located coordinate frame (A_{TCP}) are offset from the ball coordinate frame by a translation and rotation described by the homogeneous transformation matrix (HTM) $^{TCP}T_{Ball}$. The measurement system also has an attached coordinate frame (A_{MS}). When the coupling balls and grooves are placed nominally, A_{Ball} and A_{Groove}
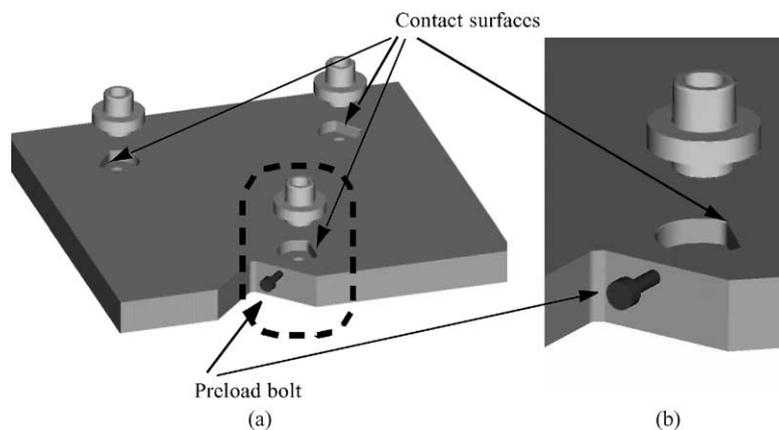

Fig. 5. Three-pin interface: (a) model of female half, with shouldered pins above (top plate not shown); (b) close view of engagement area for preloaded pin. Note that the location of contact surfaces speficied in Fig. 4b provides better interface stiffness, but the model shown here was specified by design constraints for the robot base.
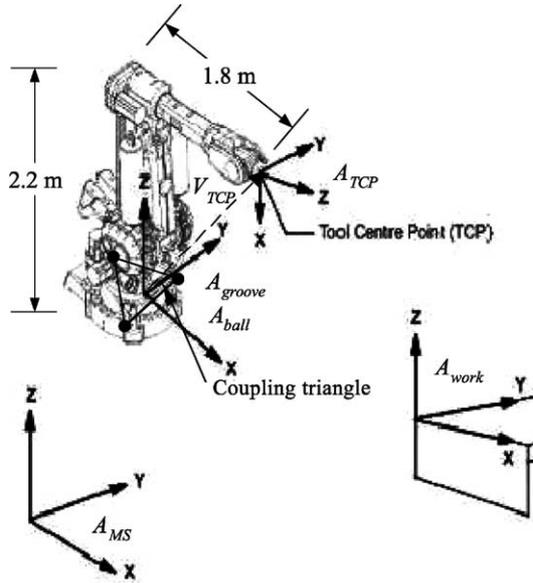
Fig. 6. Reference interface, tool, and measurement system coordinate frames with respect to kinematic couplings on the base of a robot. The ABB IRB6400R industrial manipulator is shown [12].

are coincident. Therefore, the forward kinematics of the machine are represented by $^{TCP}T_{Ball}$. Hence, when the TCP is commanded to the work location (also neglecting all errors not related to the kinematic couplings), the TCP frame and the work frame coincide, such that:

$$^{TCP}T_{Ball-nom} = {}^{Work}T_{Ball-nom}. \tag{1}$$

When error in the kinematic couplings is present, A_{Ball} and A_{Groove} become offset and Eq. (1) is invalid. The translational errors are reflected exactly at the TCP, and the rotational errors are magnified as sine and cosine errors by the distance from the base to the TCP.

3.2. Component errors

The sources of tolerance error from manufacturing and assembly variation of a kinematic interface are:

1. positional tolerances of the mounting holes in the interface plate holding the balls and in the interface plate holding the grooves;
2. flatness variation of the interface plate that holds the balls and the interface plate that holds the grooves;
3. feature and form errors in the balls and grooves; and
4. errors in press-fitting the ball and groove mounts to the coupling halves, resulting primarily in translation error normal to the mounting surfaces and angular error about the insertion axis.

In addition, if the relative placements of the kinematic couplings are measured in an attempt to estimate the tolerance errors, error in the measurement system is important. For
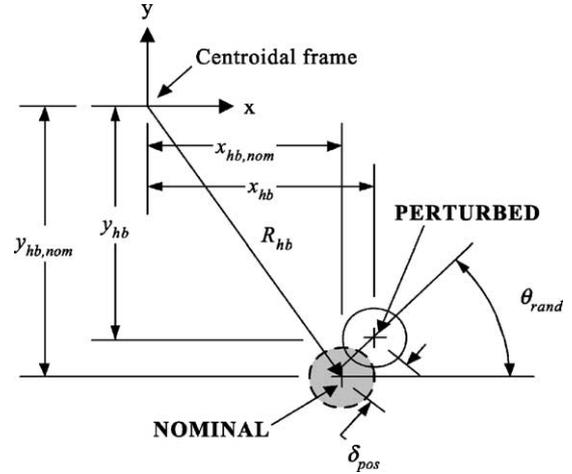

Fig. 7. Error motion of a single mounting hole with respect to the centroidal frame.

a present-day industrial laser tracker, this is a maximum of 0.01 mm/m of dead path.[2]

For example, errors in placement of the interface plate holes for mounting the kinematic couplings can be estimated by placing normal distributions within specified 3σ diametrical tolerance zones of the nominal positions of the holes. Using this method, the perturbed coordinates $(x_{h_{b1}}, y_{h_{b1}})$ of a mounting hole, shown in Fig. 7, are:

$$x_{h_{b1}} = x_{h_{b1}nom} + \delta_{pos}\text{RandN}() \cos(\theta_{rand}) \tag{2}$$

$$y_{h_{b1}} = y_{h_{b1}nom} + \delta_{pos}\text{RandN}() \sin(\theta_{rand}) \tag{3}$$

$$\theta_{rand} = 2\pi\text{Rand}(). \tag{4}$$

In these equations:

1. $(x_{h_{b_1}nom}, y_{h_{b1}nom})$ is the nominal position of the mounting hole, in the coupling plane.
2. δ_{pos} is the position tolerance of the mounting hole, expressed as the 3σ radius of a tolerance zone centered at the hole's nominal location.
3. θ_{rand} is the random angular direction along which the error motion is applied, measured counter-clockwise from the x-axis of the centroidal frame.
4. RandN() is a *normally* distributed random number between -1 and 1, which scales the radial distance of the perturbation from the nominal hole center. The normal distribution guarantees a heavier weight to smaller radial distances.
5. Rand() is a *uniformly* distributed random number between -1 and 1, used to calculate the orientation of the perturbation with respect to the coordinate frame of the interface plate. The uniform distribution guarantees an arbitrary orientation of the error.

---

[2] This excludes systematic temperature dependence, which is reasonably eliminated by built-in software correction from temperature readings [13].
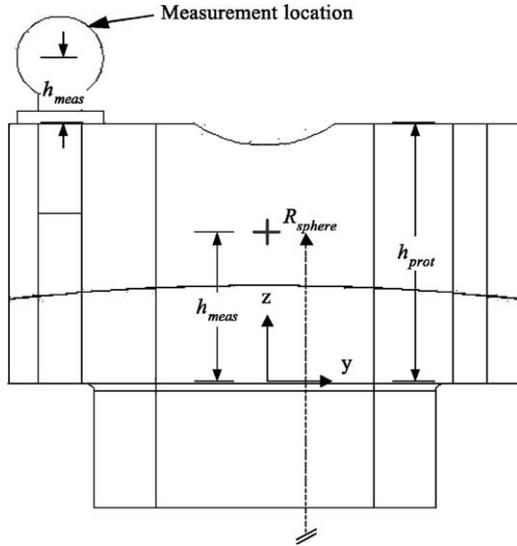
Fig. 8. Definitions of local z-direction dimensions of a canoe ball.

Similar calculations are made for variations of the interface plate thickness, coupling mounting orientation, and dead path error of the measurement system.

Furthermore, when the coupling is measured at a point offset from its contact location, form error of the coupling affects the interchangeability. To model this effect, a local coordinate system is placed at the base of the ball or groove mount, along the axis of its mounting hole, as shown in Fig. 8. The expected form error stackup between the offset measurement sphere and the ball contact point is calculated as the average of root-sum-square (RSS) and worst-case stackups of the form error components [5]. For example, the local z-direction error $\delta_{z,1}$ in the measurement estimate of the location of the canoe sphere contact point is:[3]

$$\delta_{z,1} = \frac{1}{2}\left[\left(2\left(\frac{\delta_{\mathrm{Rsph}}}{\sqrt{2}}\right) + \delta_{\mathrm{hR}} + \delta_{\mathrm{hprot}} + \delta_{\mathrm{hmeas}}\right) \right.$$
$$\left. + \sqrt{2\left(\frac{\delta_{\mathrm{Rsph}}}{\sqrt{2}}\right)^2 + \delta_{\mathrm{hR}}^2 + \delta_{\mathrm{hprot}}^2 + \delta_{\mathrm{hmeas}}^2} \right], \quad (5)$$

where δ_{Rsph} is the radius tolerance of the contact sphere, δ_{hR} is the tolerance of the contact point relative to the bottom of the bulk protrusion, along the z-axis, δ_{hprot} is the height tolerance of the canoe ball, and δ_{hmeas} is the height tolerance of the measurement feature relative to the canoe ball.

3.3. Combination of errors

The propagation of errors in the interface components to a total error at the TCP is shown by the block diagram in Fig. 9. First, the nominal geometries of the interface plates, the kinematic couplings, and the measurement feature are specified.

The perturbations in mounting hole placement, machined form of the kinematic couplings, and of the inserted tooling ball measurement feature (discussed in the next section), are introduced. Insertion errors occur between the measurement features and the kinematic couplings, and between the kinematic couplings and the interface plates. The total error is derived from the sum[4] of the component errors at each of the contact points, and is expressed as a transformation matrix between the nominal and true centroidal frames of each interface half. These matrices, calculated using measurements of the contact points before the interface halves are mated, are denoted $^{\mathrm{Ball\text{-}true}}T_{\mathrm{Ball\text{-}nom}}$ and $^{\mathrm{Groove\text{-}true}}T_{\mathrm{Groove\text{-}nom}}$, and are specified to a model of the kinematic constraints between the balls and grooves. This model calculates the mating error between the centroidal frames as a third error transformation, $^{\mathrm{Ball\text{-}true}}T_{\mathrm{Groove\text{-}true}}$.

The interface transformation ($^{\mathrm{Ball\text{-}nom}}T_{\mathrm{Groove\text{-}nom}}$) accounts for the total interchangeability error between the kinematic coupling balls and grooves; hence, it expresses the relationship between the nominal centroidal frame of the grooves (referenced to other objects in the cell) and the nominal centroidal frame of the balls (referenced to the machine structure), expressed in the coordinate frame of the measurement system:

$$^{\mathrm{Ball\text{-}nom}}T_{\mathrm{Groove\text{-}nom}} = (^{\mathrm{Ball\text{-}true}}T_{\mathrm{Ball\text{-}nom}})^{-1}\,{}^{\mathrm{Ball\text{-}true}}$$
$$T_{\mathrm{Groove\text{-}true}}\,{}^{\mathrm{Groove\text{-}true}}T_{\mathrm{Groove\text{-}nom}}. \quad (6)$$

This transformation[5] can be added to the forward kinematics of the machine to reduce the interchangeability error at the TCP.

To relate the interchangeability error at the interface to the error at the TCP, first recall that if the tolerance errors at the interface are zero, this model will predict that the stationary work frame (A_{Work}) and the frame at the TCP (A_{TCP}) are coincident. When tolerance errors are introduced without appropriate correction of the machine's work location, there will be a mismatch between the work and TCP frames, given by the transformation:

$$^{\mathrm{Work}}T_{\mathrm{TCP}} = (^{\mathrm{TCP}}T_{\mathrm{Ball\text{-}nom}}\,{}^{\mathrm{Ball\text{-}nom}}T_{\mathrm{Groove\text{-}nom}})^{-1\,\mathrm{Work}}$$
$$\times\, T_{\mathrm{Ball\text{-}nom}}. \quad (7)$$

Then, the vector giving the interchangeability error at the TCP is:

$$E_{\mathrm{TCP}} = {}^{\mathrm{TCP}}T_{\mathrm{Ball\text{-}nom}}\,{}^{\mathrm{Ball\text{-}nom}}T_{\mathrm{Groove\text{-}nom}}V_{\mathrm{TCP}}, \quad (8)$$

where V_{TCP} is the vector from the origin of A_{Ball} to the (nominal) origin of A_{TCP}. This vector goes from the desired work

---

[3] The effective radius tolerance is doubled in Eq. (4) because there are two spherical surfaces per coupling mount.

[4] As in Eq. (5) the average of the RSS and worst-case sums is taken.

[5] Note that Fig. 9 distinguishes between the perfect interface transformation ($^{\mathrm{True,Ball\text{-}nom}}T_{\mathrm{True,Groove\text{-}nom}}$) which would give zero residual error at the TCP and the interface transformation calculated from measurements ($^{\mathrm{Ball\text{-}nom}}T_{\mathrm{Groove\text{-}nom}}$). Hence, the residual error at the TCP comes from error in measuring the kinematic couplings, and in practice also from errors excluded from this model.
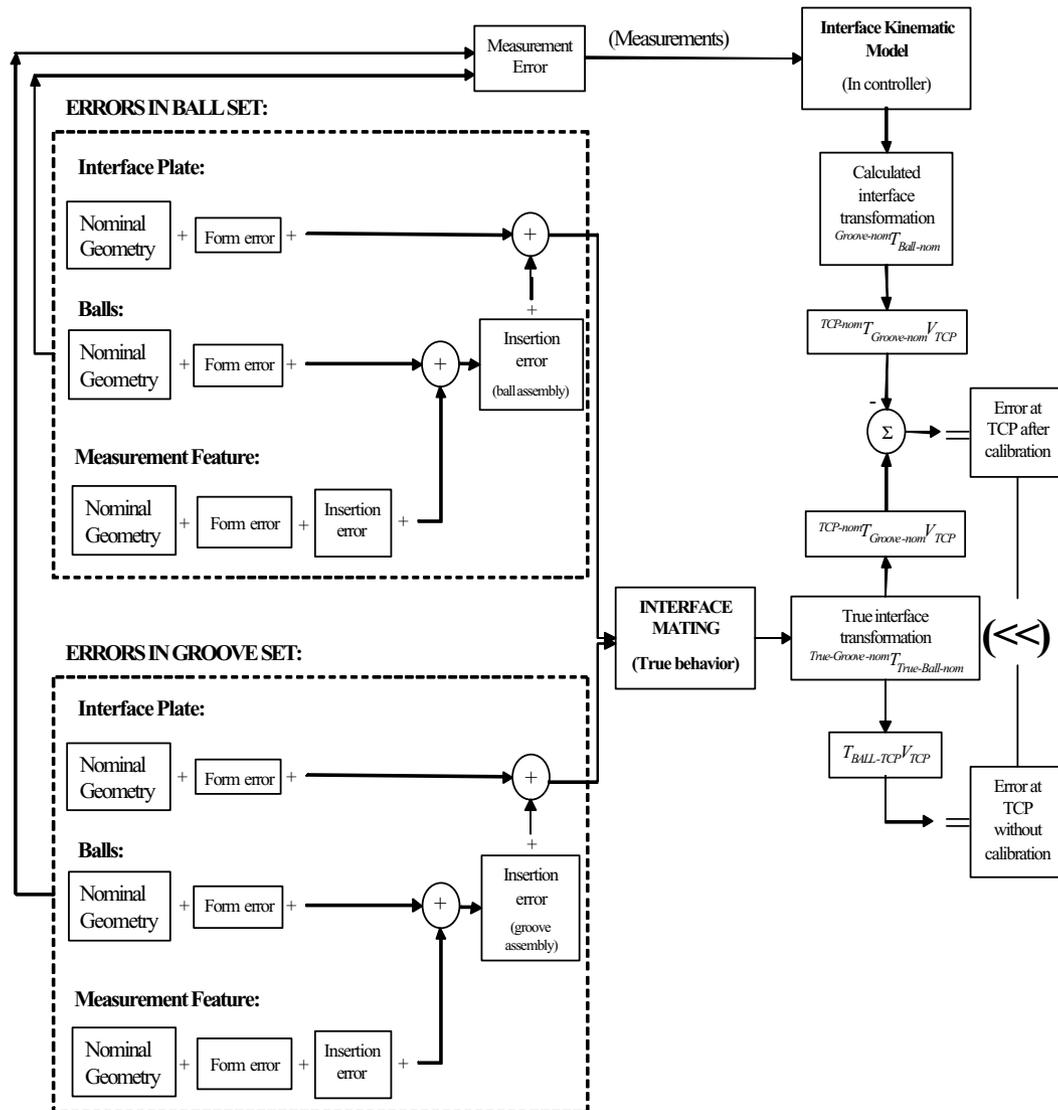
Fig. 9. Interchangeability error stackup for a kinematic coupling.

point to the true TCP location found by considering the interchangeability error. The next section describes the procedure for deriving the interface transformation directly from the measured locations of the coupling balls and grooves.

4. Solution method for interface calibration

When mounting an interface in practice, the errors between the ideal (nominal) and real centroidal frames of the interface halves can be estimated by measuring appropriate features of the balls and grooves. Knowing the ideal positions of the contact surfaces, the measured positions are inputs to a kinematic model of the interface geometry which predicts $^{\text{Ball-nom}}T_{\text{Groove-nom}}$. This section presents and validates of an interchangeability model for canoe ball couplings. A model of the three-pin interface was also built, with simplification of the contact constraints to give a deterministic seating po-

sition. A brief discussion of this model is in Appendix A and the reader is referred to Hart [4] for more details.

4.1. Canoe ball interface model

When contact surfaces or offset features such as tooling balls of kinematic couplings are measured, the geometric mating relationship between the centroidal frames of the interface halves is found by solving a system of 24 linear equations. Specifically, measurement of the canoe ball interface gives location estimates[6] for the following features of the

---

[6] When an offset feature such as a tooling ball is measured, these values are predicted based on the nominal geometry of the coupling. Eq. (5) gives error of this prediction in addition to the error of the measurement system. An example of direct measurement is taking multi-point measurements of the spherical surfaces of the canoe balls and the vee flats of the grooves. In this case, the error of the predictions is solely the error of the measurement system, including the fitting algorithms.
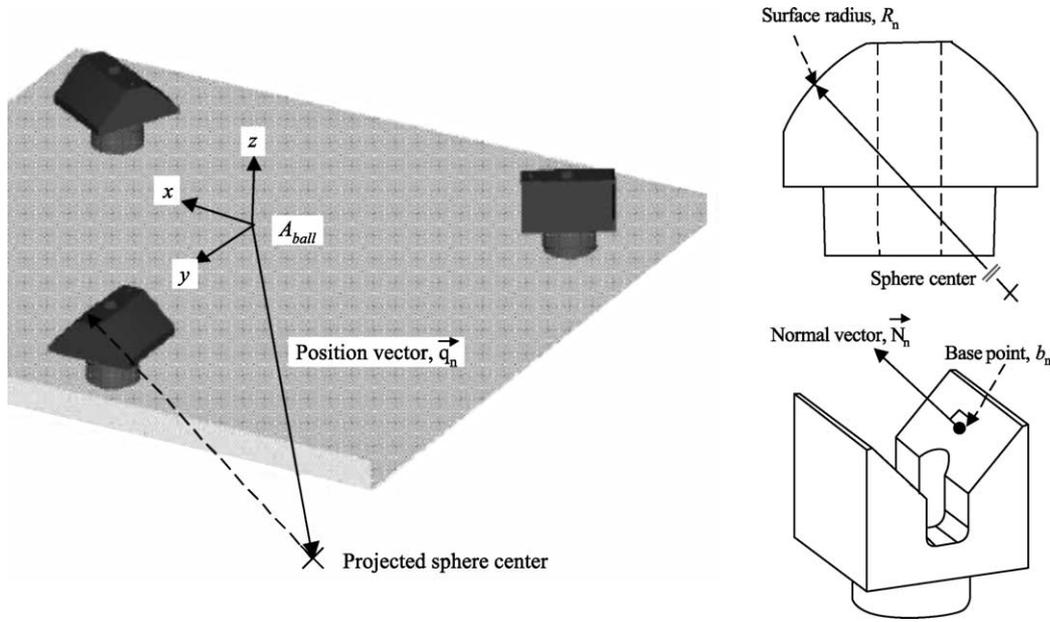
Fig. 10. Measured parameters of canoe balls and vee grooves.

balls and grooves:

1. $[R_1, \ldots, R_6]$: The radii of the six spherical contact surfaces.
2. $[\vec{q}_{S1}, \ldots, \vec{q}_{S6}]$: Position vectors[7] directed from each sphere center to the centroid of the ball interface. For example, $\vec{q}_{S1} = \langle u_{Sn1}, v_{Sn1}, w_{Sn1} \rangle$.
3. $[b_1, \ldots, b_6]$: The base points of the six groove flats, relative to the measurement frame (A_{MS}). For example, $b_1 = (x_{b1}, y_{b1}, z_{b1})$.
4. $[\vec{N}_1, \ldots, \vec{N}_6]$: Normal vectors to the six groove flats, in A_{MS}. For example, $\vec{N}_1 = \langle x_{N1}, y_{N1}, z_{N1} \rangle$.

These features are shown in Fig. 10. The six unknown rest positions (18 unknown coordinates) of the sphere centers are denoted $[p_{S1}, \ldots, p_{S6}] = [(x_{S1}, y_{S1}, z_{S1}), \ldots, (x_{S6}, y_{S6}, z_{S6})]$. The remaining six unknowns are the six error offsets between the centroidal frames of the interface plates, $[\varepsilon_x, \varepsilon_y, \varepsilon_z, \theta_x, \theta_y, \theta_z]$.

Separating variable and constant coefficients, the system has the matrix form $AX = B$, where X is the 24-element vector containing the unknown final coordinates of the spheres with respect to the measurement system and the six error motions of the interface. The components of the 24×24 matrix A and the 24-element column vector B will be apparent from the equations discussed shortly. After inverting A and multiplying the result by B, the six error motions between the centroidal frames are elements of X. With small angle approximations, the transformation between centroidal frames is then:

$$^{\text{Ball-true}}T_{\text{Groove-ture}} = \begin{bmatrix} 1 & -\theta_{z_c} & \theta_{y_c} & \delta_{x_c} \\ -\theta_{z_c} & 1 & -\theta_{x_c} & \delta_{y_c} \\ -\theta_{y_c} & \theta_{x_c} & 1 & \delta_{z_c} \\ 0 & 0 & 0 & 1 \end{bmatrix}. \qquad (9)$$

$^{\text{Ball-nom}}T_{\text{Groove-nom}}$ is calculated by combining this result with $^{\text{Ball-true}}T_{\text{Ball-nom}}$ and $^{\text{Groove-true}}T_{\text{Groove-nom}}$ (known directly from the measurements) according to Eq. (6). Then, given a kinematic model of the machine, the error vector is found using Eq. (8).

To construct the system of equations, first consider that when the interface is seated, the projected center of each spherical surface will be as close as possible to its mating groove. Hence, the line passing through the projected center of the each sphere and the contact point between the sphere and its mating groove flat will be normal to the flat. Then, the distance between the projected sphere center and the groove flat is equal to the measured radius of the spherical surface. For example, the mathematical constraint between the first sphere and mating flat for the first canoe ball to groove pair, with unknown p_1, is:

$$\frac{(p_1 - b_1) \cdot \vec{N}_1}{\| \vec{N}_1 \|} = R_1. \qquad (10)$$

A group of six similar equations, one for each sphere/flat pair, contains the 18 final coordinates of the sphere centers as unknowns.

Second, the measured distances between the sphere centers, represented by $[\vec{q}_{S1}, \ldots, \vec{q}_{S6}]$, must not change. The motions $[\varepsilon_x, \varepsilon_y, \varepsilon_z, \theta_x, \theta_y, \theta_z]$ of the centroidal frame of the ball interface (A_{Ball}) with respect to centroidal frame of

---

[7] These can be expressed in an arbitrary coordinate frame; only the distances between the ball centers are important. The simulation model expresses the position vectors with respect to the centroidal ball frame (F_{Ball}).
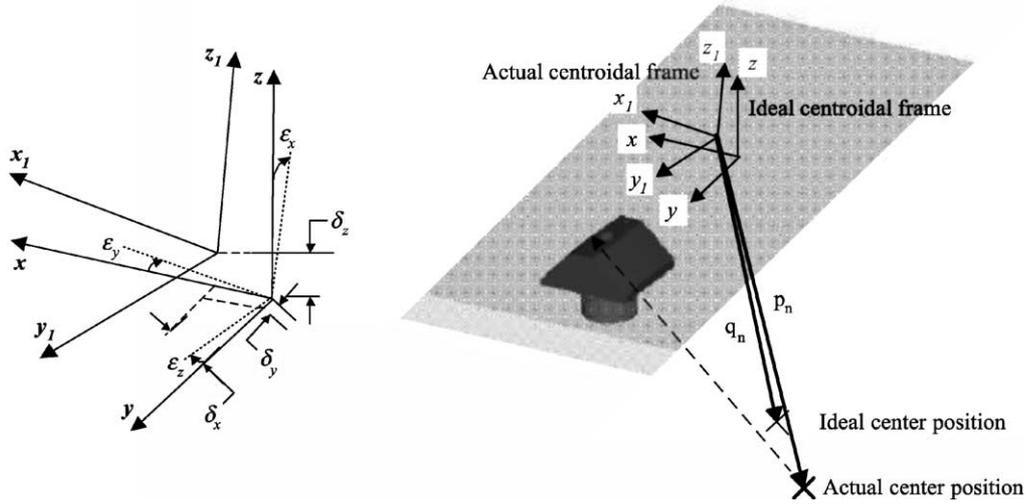
Frame error motions:

Fig. 11. Relationship between error motions of centroidal frame and offset sphere center.
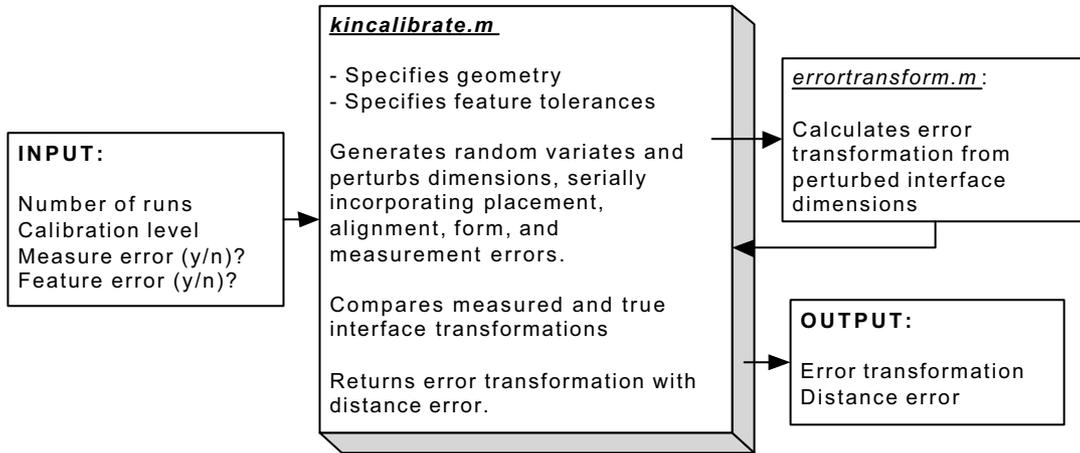

Fig. 12. Structure of MATLAB^{TM} model for kinematic coupling interchangeability analysis.

the groove interface (A_{Groove}), can be expressed in terms of the final positions of the sphere centers. For example, the final position of the first sphere center is:[8]

$$x_{S1} = \delta_{x_c} + u_{S1}[c(\theta_{z_c})c(\theta_{y_c})]$$
$$+ v_{S1}[c(\theta_{z_c})s(\theta_{y_c})s(\theta_{x_c}) - s(\theta_{z_c})c(\theta_{x_c})]$$
$$+ w_{S1}[c(\theta_{z_c})s(\theta_{y_c})c(\theta_{x_c}) - s(\theta_{z_c})s(\theta_{x_c})] \quad (11)$$

$$y_{S1} = \delta_{y_c} + u_{S1}[s(\theta_{z_c})c(\theta_{y_c})]$$
$$+ v_{S1}[s(\theta_{z_c})s(\theta_{y_c})s(\theta_{x_c}) - c(\theta_{z_c})c(\theta_{x_c})]$$
$$+ w_{S1}[s(\theta_{z_c})s(\theta_{y_c})c(\theta_{x_c}) - c(\theta_{z_c})s(\theta_{x_c})] \quad (12)$$

$$z_{S1} = \delta_{z_c} + u_{S1}[-s(\theta_{y_c})]$$
$$+ v_{S1}[c(\theta_{z_c})s(\theta_{x_c})]$$
$$+ w_{S1}[c(\theta_{y_c})c(\theta_{x_c})]. \quad (13)$$

---

[8] The operation $s(\cdot)$ denotes $\sin(\cdot)$ and $c(\cdot)$ denotes $\cos(\cdot)$.

In order to calculate the matrices A and B, small angle approximations must be made such that:

$$x_{S1} = \delta_{x_c} + u_{S1} - v_{S1}\theta_{z_c} + w_{S1}\theta_{y_c} \quad (14)$$

$$y_{S1} = \delta_{y_c} + u_{S1}\theta_{z_c} + v_{S1} - w_{S1}\theta_{x_c} \quad (15)$$

$$z_{S1} = \delta_{y_c} - u_{S1}\theta_{y_c} + v_{S1}\theta_{x_c} + w_{S1}. \quad (16)$$

These relationships are diagrammed in Fig. 11. Taken for the position of each sphere, they are the final 18 equations of the system.

Therefore, the matrix of coefficients A contains the components of the six groove normal vectors (as in Eq. (11)) in its upper six rows, and the centroidal position vectors $[\vec{q}_{S1}, \ldots, \vec{q}_{S6}]$ (components as in Eqs. (12)–(14)) of the ball centers in its lower 18 rows. The constant vector B contains the projections of the groove normal vectors along the position vectors $[\vec{q}_{S1}, \ldots, \vec{q}_{S6}]$ as its upper six elements, and the constant terms in the centroidal error motion equations as its lower 18 elements.

Table 1
Calibration options for canoe ball interface when offset features are measured

Complexity	Example calibration procedure
0	Measure nothing, assuming nominal geometry
1	Measure the position of a single tooling ball on each vee groove
2	In addition to (1), measure the center location of the bolt hole in each vee groove. This enables calculation of the vee groove orientations
3	In addition to (2), measure the position of a single tooling ball on each canoe ball
4	Measure single tooling balls on each canoe ball and vee groove
5	In addition to (3), measure the center location of the bolt hole in each canoe ball. This enables calculation of the canoe ball orientations

Table 2
Calibration options for canoe ball interface when contact surfaces are measured directly

Complexity	Example calibration procedure
0	Measure nothing, assuming fully nominal placement
1	Perform a sphere fit to the curved surfaces of each canoe ball, calculating center positions and radii
2	Perform a three-point plane fit to each vee groove flat, calculating base points and normal vectors
3	Combine (2) and (3)

4.2. Simulation model

The interchangeability model was built as a series of MATLAB™ scripts, structured as shown in Fig. 12. Parameters within the scripts specify the nominal geometry and error tolerance values. Given this information, the model predicts the average interchangeability error at the TCP for a variety of levels of calibration detail. For calibration of canoe ball interfaces including tooling balls as offset measurement features, the six levels of calibration listed in Table 1 are identified. When the contact surfaces are measured directly, the three levels of calibration listed in Table 2 are tested. Simulation results for each of the calibration complexity levels are presented for the industrial robot base in Section 5. The reader is encouraged to download[9] the MATLAB scripts to follow the mathematical calibration routine and demonstrate the interchangeability model.

4.3. Physical experiments

The canoe ball interchangeability model was validated by building a series of small prototype models and measuring the error in the positions and orientations of their centroidal frames over all possible combinations of ball sets and groove sets. A large baseplate had two arrangements of six grooves spaced at equal 60° angles around a center point. Ten smaller top pallets were also manufactured, each with an equilateral arrangement of canoe balls. To ensure statistical confidence in the calibration-interchangeability relationship, the locations of the coupling mounting and alignment hole pairs on each

[9] The scripts can be downloaded from the tools section of http://pergatory.mit.edu/kinematiccouplings.

plate were intentionally perturbed within circular tolerances zones of 0.64 mm (3σ diameter) from their nominal positions. Reference measurement spheres were placed at identical positions with respect to the coupling centroids on the pallets and baseplate.

Fig. 13 shows the setup while it was being measured on a Brown & Sharpe MicroVal PFX CMM. The measurement spheres of each pallet were measured in each mounting configuration, and after applying the known offsets between the sphere locations and the nominal coupling locations, the interface transformation was calculated by directly specifying the measured positions of the contact points to the algorithm discussed in the previous section.

Fig. 14 plots the in-plane angular error of each interface combination (choice of a pallet, groove set on the baseplate, and relative orientation), as measured between the centroidal frames, and after the transformation correction was applied to the measurements. The combinations are grouped for each of the five pallets. The fifth pallet, for which the interchangeability correction actually increases the error for some trials, was machined with no more than 0.01 mm deviation from the nominal mounting hole locations. Over all trials, applying the interface transformation reduced the placement error by an average of 92%, specifically from 1.5×10^{-3} to 1.4×10^{-4} rad for in-plane rotation. The average total error (positional error plus sine and cosine errors) reported at a 100 mm circle from the coupling centroid was then 0.015 mm, which was within
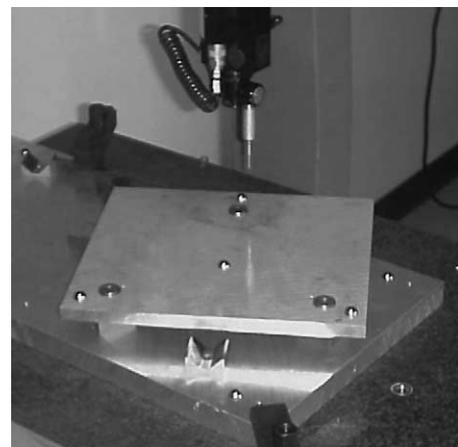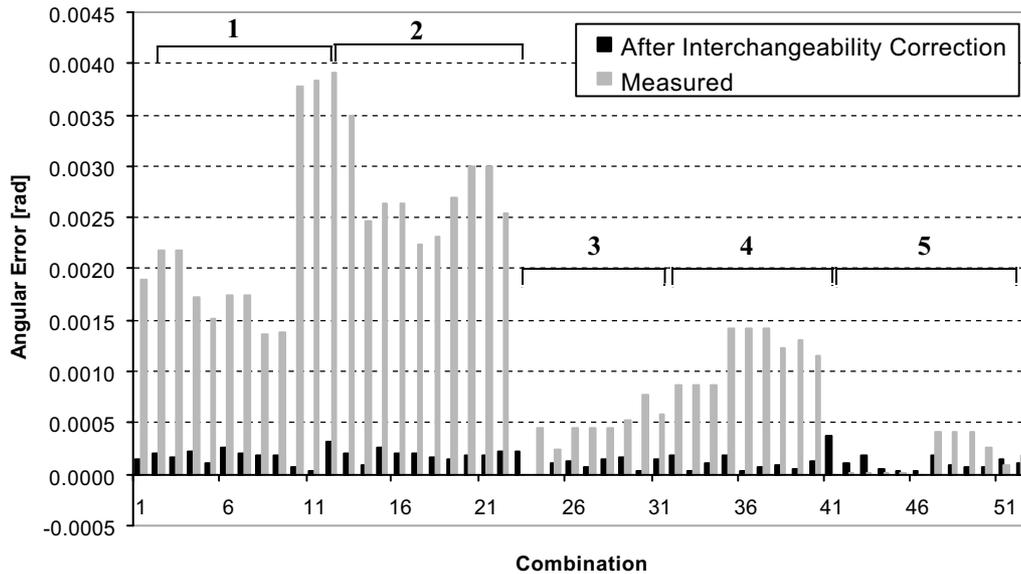

Fig. 13. Interchangeability measurement setup.

Fig. 14. In-plane angular error of prototype pallets (numbered groups) before and after transformation correction.

the accuracy limits imposed by the CMM and the tooling ball placements by CNC machining[10] and a light press-fit.

5. Application to industrial robots

5.1. Coupling designs

Kinematic couplings were designed for the base and wrist interfaces of an ABB IRB6400R six-axis industrial robot manipulator, shown in Fig. 15. The base interface sits between the robot foot and the factory floor, and is normally restrained with eight 20 mm diameter bolts. The new three-bolt alternatives are a canoe ball interface (shown in Fig. 16), a three-pin interface, and a groove–cylinder interface (see [4] for details). The interface between the robot wrist (the module providing the fifth and sixth rotational motions) and the robot arm is normally restrained with eight bolts clamping friction-holding plates between planar contact surfaces. New wrist mountings were designed using canoe ball couplings, and a three-pin coupling (shown in Fig. 17).

5.2. Repeatability performance

The repeatability of the base and wrist interfaces was measured using a Leica LTD500 Laser Tracker [13], which is traditionally used for calibration of the IRB6400R. A "cat's eye" retroreflector was mounted at the robot TCP, and static measurements were taken at five points in the robot's workspace. In each case, the interface was fully dismounted and re-

mounted between measurement trials, giving the average repeatability values shown in Figs. 18 and 19.

The repeatability of the canoe ball base and wrist mountings in the shop environment is noticeably much higher than would be expected based on documented laboratory measurements of kinematic couplings, notwithstanding the large amplification in angular errors seen by taking measurements at the robot TCP. This emphasizes several implications for
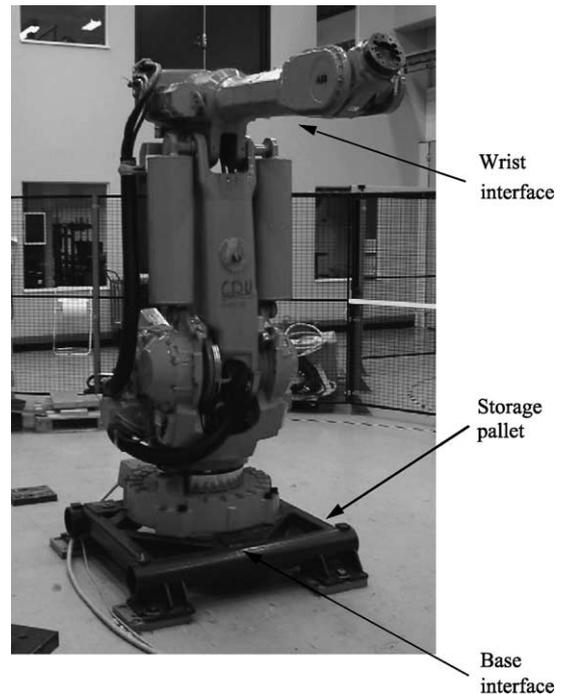

Fig. 15. ABB IRB6400R. Base of manipulator shown is conventionally mounted using two-pin locators and eight bolts. The pallet shown is bolted to anchors in the floor.

---

[10] Error of the CNC machine used to machine the plates was approximately 0.05 mm/m of travel, more than an order of magnitude below the prescribed perturbations for the mounting holes.
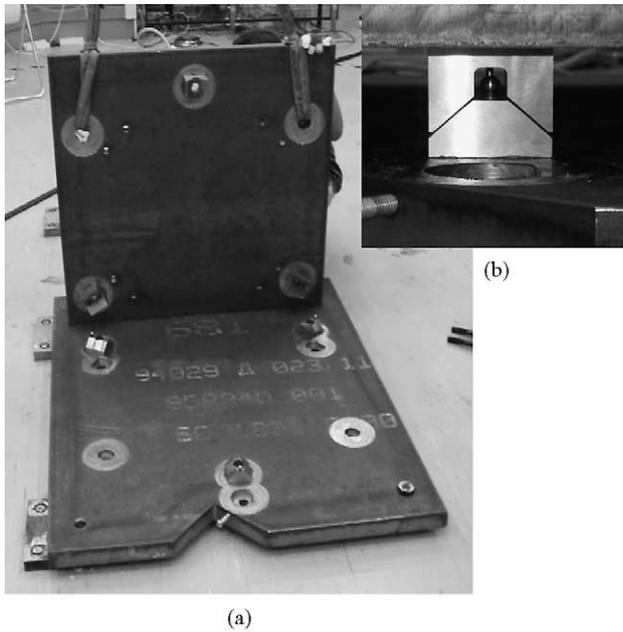
Fig. 16. Prototype canoe ball kinematic coupling interface plates for industrial robot base mounting: (a) plates after coupling insertion; (b) close view of single coupling with tooling ball for calibration. Production design would machine grooves directly to robot foot, and place balls in floor-mounted baseplate.

mounting kinematic couplings in high-load industrial situations, such as:

1. Bolt preload should be applied incrementally using a torque gauge wrench, while bolts should be greased and contacts should be cleaned between mountings. A factor of at least 2:1 improvement in repeatability of the robot base was observed when the mounting procedure was refined in this fashion.
2. Interfaces should be engaged as gently as possible, with initial contact as close to the final seating position as possible. It was extremely difficult to seat the robot manipulator on its base without initial offset, increasing the sliding distance needed to reach the seating position. Dithering

the interface with low-frequency vibration before tightening the bolts is recommended.
3. As shown by the wrist results, installation orientation is also important. For an equal-angle, in-plane kinematic coupling as was tested, installation with the couplings in the horizontal plane is best. Other groove configurations, some discussed in Slocum [5], should be investigated when horizontal mounting is not possible.

5.3. Interchangeability simulations

Interchangeability simulations were conducted for the base and wrist interfaces interface, specifying the geometry of the manufactured prototypes and manufacturing and assembly tolerances representative of high volume production of the components. Ten thousand iterations were conducted for each level of calibration complexity listed in Section 4.2.

Fig. 20 shows the simulation results for the base interface. The model predicts that the interface transformation accounts for approximately 50% or 0.11 mm of the 0.22 mm average total interchangeability error when full calibration is performed relative to offset measurement features. When the contact surfaces are measured directly, the interchangeability analysis reduces the tool point error by 88% to 0.02 mm. In the latter case the remaining error is solely due to measurement error; in the former case, variation in the dimension and placement of the measurement feature is also a factor. A negligible advantage in accuracy is gained by knowledge of the relative orientations of the balls and grooves. Hence, unless the process of mounting the couplings to the plates is poorly controlled, only measurement of a single feature is needed for very good calibration performance when offset measurement is performed.

5.4. Estimates of total mounting error

Best-case measured repeatability values for the base and wrist canoe ball designs are added to simulated interchangeability values with full calibration to give the estimates of total error reported in Table 3. Overall, the accuracy benefit of
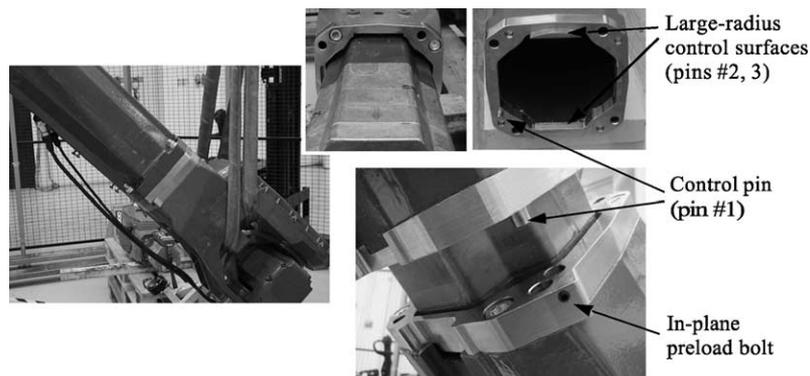

Fig. 17. Prototype three-pin coupling for mounting robot wrist to robot arm. In-plane preload is applied to the bolt indicated; four normal-to-plane bolts provide dynamic stiffness.
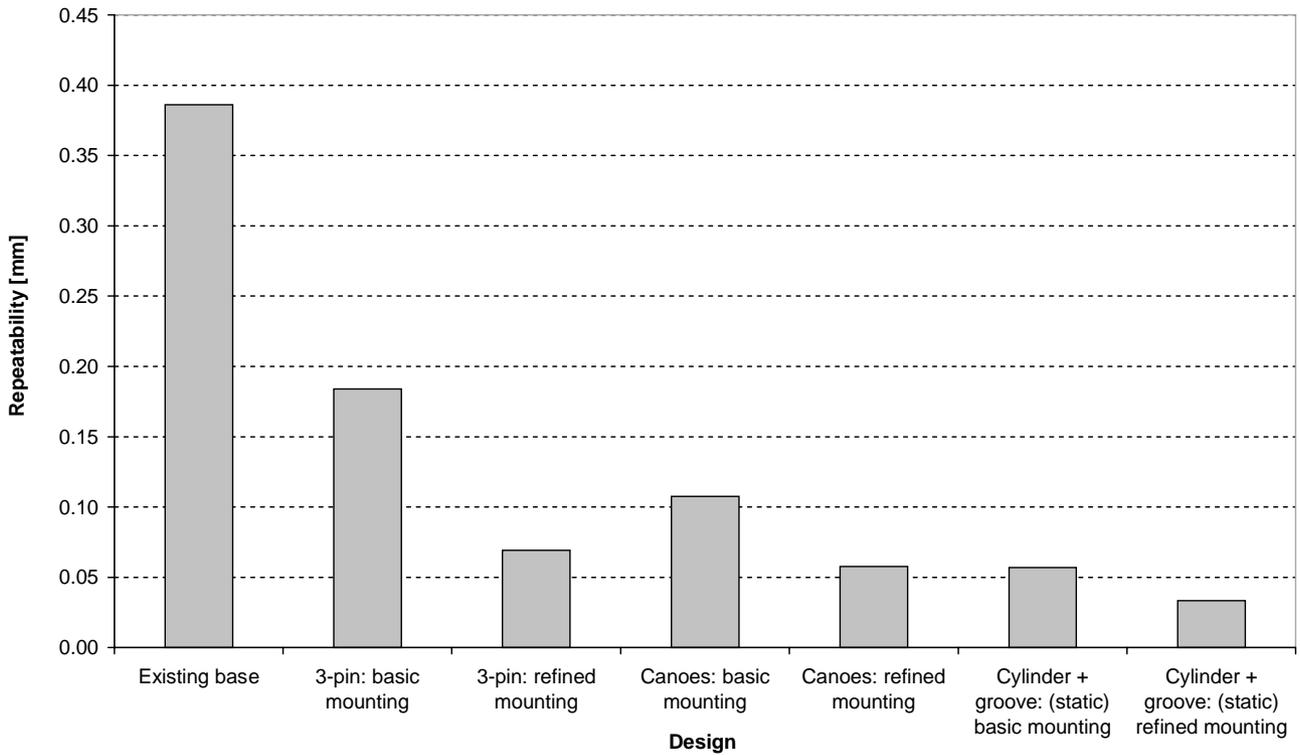
Fig. 18. Repeatability measurements of kinematic coupling robot base mountings. Basic mounting procedure was to tighten bolts sequentially using a wrench, applying full preload torque to each at once. Refined mounting procedure was to incrementally (10, 50, 100% of 300 N m limit) tighten the bolts in sequence using a torque wrench, and clean the coupling contacts and grease the bolts between trials.
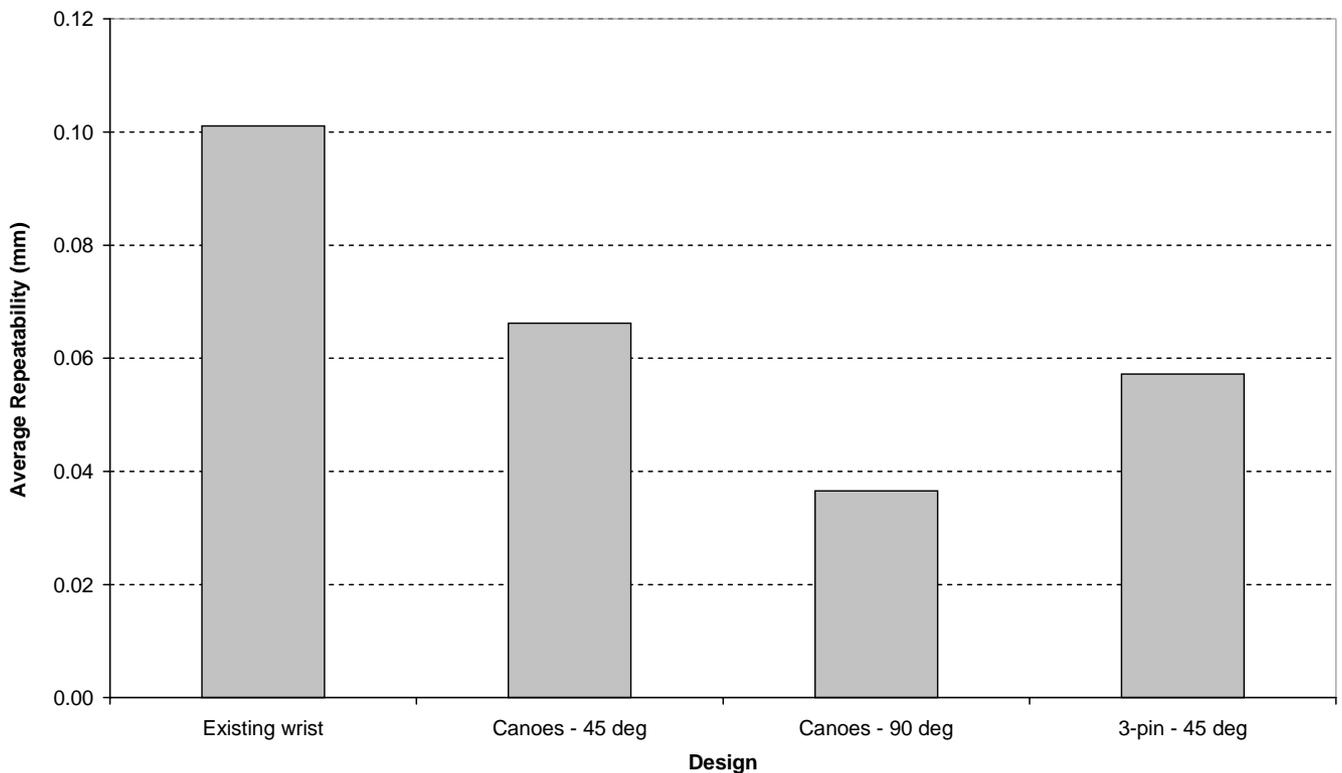

Fig. 19. Repeatability measurements of kinematic coupling robot wrist mountings. Willoughby [7] presents data for several additional combinations of preload and mounting configuration. Mounting angle is measured between the robot arm and the floor. Three-pin measurements at 90° are not presented because the interface was damaged.

Table 3
Estimated total accuracy of kinematic coupling designs for robot base and wrist

Interface	Average repeatability (Figs. 18 and 19)	Average interchangeability (simulated)	Total accuracy (mm)
Wrist, canoe balls—offset	0.06	0.03	0.09
Wrist, canoe balls—direct	0.06	0.01	0.07
Wrist, three-pin—direct	0.07	0.01	0.08
Base, canoe balls—offset	0.06	0.12	0.18
Base, canoe balls—direct	0.06	0.03	0.09
Base, three-pin—direct	0.07	0.03	0.10

"Offset" designation refers to interchangeability simulation conducted for an offset measurement feature; "direct" simulates measurement of the coupling contact surfaces.

using a precision-machined canoe ball setup is negligible over the simple three-pin interface based on the measurement results here. Cost of the custom-manufactured canoe balls (US$ 1000–3000 per three balls and grooves, depending on size, in a quantity of 100) would make them prohibitive for most industrial applications based on cost-performance considerations. A promising industrial alternative to the designs presented may be found in conical line contact quasi-kinematic couplings designed by Culpepper [14], which were applied
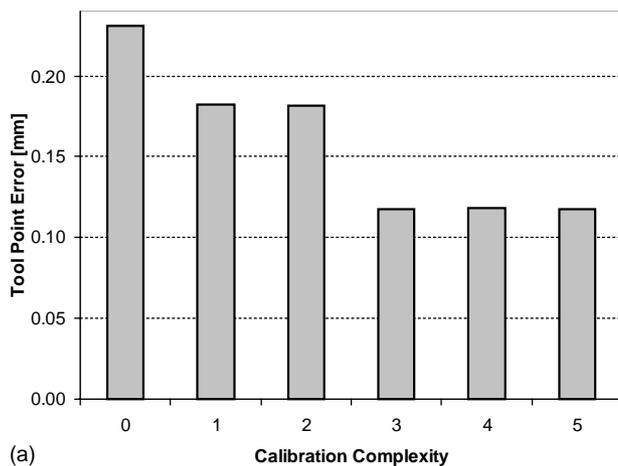

Fig. 20. Predicted interchangeability error at TCP vs. interface calibration detail for robot base: (a) calibration by measurement of offset measurement sphere and bolt hole; (b) calibration by measurement of spherical surfaces and groove flats.

to the mating halves of an automotive engine block for repeatable location during successive machining operations.

6. Conclusions

Direct measurement of the contact points on the halves of a kinematic interface can greatly reduce the effect of tolerance errors on mounting accuracy, with the residual interchangeability error based only on the error of the measurement procedure. By estimating the total mounting accuracy of a kinematic coupling as the sum of the measured repeatability and the simulated interchangeability, interface manufacturing tolerances and the complexity of the calibration process can be chosen to satisfy an accuracy requirement at minimum cost. While past laboratory measurements of kinematic couplings have shown micron-level repeatability at relatively small scales, a test application to industrial robot base and wrist mountings shows that measured repeatability error is approximately equal to interchangeability error derived from simulation. These results show that when interfaces experience heavy loads, and when variability in bolt preload, cleanliness of the contacts, and mating procedure is present, a quasi-kinematic coupling such as the three-pin interface may offer equal performance to a ball–groove coupling, at much lower cost.

In both cases, the interface transformation has the potential to become a universal kinematic handshake between kinematically coupled objects, and could enable a conceptually new interface-centric calibration process for modular machines, whereby:

1. Interface halves are pre-assembled and encoded with their coupling calibration information, relative to their centroidal coordinate frames.
2. These calibrated interface halves are attached to machine modules (e.g. robot foot), and the modules are calibrated by mounting the assembly to a reference mating interface half. The coupling parameters of the reference interface are known; hence a calibration $^{\text{Ball-nom}}T_{\text{Groove-nom}}$ is known.
3. When the machine modules are brought to the production installation site, the production interface transformation is calculated from the coupling parameters of both production interfaces. A correction is applied to the
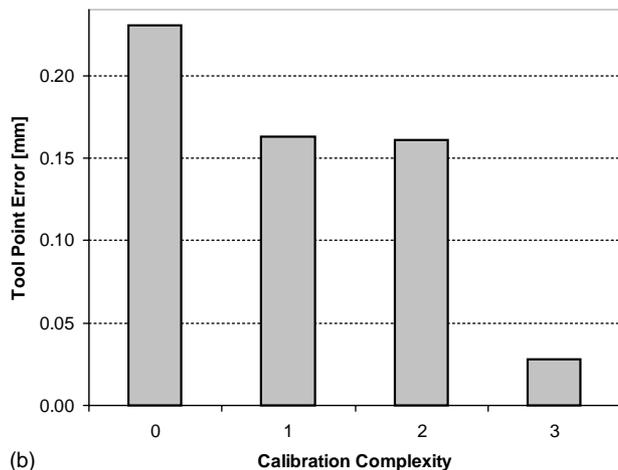
machine module calibration for the difference between the calibration $^{\text{Ball-nom}}T_{\text{Groove-nom}}$ and the production $^{\text{Ball-nom}}T_{\text{Groove-nom}}$. This would allow the machine to be more accurately programmed off-line.

In production, by making the contact surface measurements ahead of time, calculation of $^{\text{Ball-nom}}T_{\text{Groove-nom}}$ would be a step of the machine calibration routine. Ideally, the software would take the measurement values for the components, calculate the interface HTM, and apply it to the global serial chain of transformations for the machine kinematics. The pre-measured placements of the contacts could be written to an identification tag on the interface, or the interface serial number could serve as a database key to the calibration data.

To this end, a design tool synthesizing measured repeatability trends from large body of published measurements and including interchangeability models, would be useful to engineers in application of kinematic couplings to high volume machinery products such as industrial robots. In beginning such an effort, a comprehensive archive of literature and design tools for kinematic couplings is kept at http://pergatory. mit.edu/kinematiccouplings. The reader is encouraged to contribute to this repository.

Acknowledgments

Appendix A. Three-pin interchangeability model

The three-pin interface model considers in-plane location by forcing three vertical pins against three vertical contact surfaces, and vertical seating by engagement of preloaded horizontal contact surfaces. Measurement of a three-pin interface gives estimates of:

1. the radii of the three-pins;
2. the in-plane positions of the pin centers, relative to the centroidal frame for the three-pins;
3. the heights of the normal contact surfaces (e.g. pin shoulders) around the pins;
4. the positions (base points) of the flat contact surfaces to which the pins mate; and
5. the normal vectors to the contact structures.

A system of nine linear equations gives the centroidal error motions of a three-pin interface when parameters of its pins and contact surfaces are perturbed:

1. Three in-plane constraints are established between the measured pin centers and the contact surfaces in the bottom plates. Similar to the method for the canoe balls, but here in two dimensions, the lines connecting contact points with the respective pin centers are parallel to the measured normal vectors of the contact surfaces.
2. Six in-plane individual coordinate constraints are established between the pin centers and the error motions of the nominal centroidal frame of the pin arrangement. These equations are identical to Eqs. (14)–(16) for the canoe ball interface.
3. After the system is solved, out-of-plane error is incorporated by adding and averaging the vertical offsets of the normal contact surfaces around the pins and on the mating plate.

However, because the three vertical line contacts and three horizontal plane contacts make the three-pin arrangement quasi-kinematic, the following assumptions are made to estimate the interface transformation:

1. The vertical contacting surfaces of the pins are perfectly parallel to the mating vertical cuts in the bottom interface plate.
2. The horizontal contact surfaces surrounding the pins in the top interface assembly are all parallel to the horizontal contact surfaces on the top of the bottom interface plate. While vertical perturbations of the locations of the horizontal contact surfaces are modeled, resulting angular errors between the contact pairs imposed by mating of all three randomly offset pairs at once are ignored.
3. Sufficient preload is always applied to perfectly seat the interface, and manufacturing variation in the location of the preload has no effect on the interface mating behavior.

A further discussion and a presentation of simulation results is found in Hart [4].

References

[1] Slocum AH, Donmez A. Kinematic couplings for precision fixturing—Part 2: Experimental determination of repeatability and stiffness. Prec Eng 1988;10:115–22.

[2] Muller-Held B. Prinzips der kinematischen Kopplung als Schnittstelle zwischen Spindel und Schleifscheibe mit praktischer Erprobung im Vergleich zum Kegel-Hohlschaft (Translation: Application of kinematic couplings to a grinding wheel interface). S.M. thesis, University of Aachen, Germany; 1999.

[3] Poovey T, Holmes M, Trumper DL. A kinematically-coupled magnetic bearing test fixture. Prec Eng 1994;16:99–108.

[4] Hart AJ. Design and analysis of kinematic couplings for modular machine and instrumentation structures. S.M. thesis, Department of Mechanical Engineering, Massachusetts Institute of Technology; 2001.

[5] Slocum AH. Precision machine design. Soc. Manufact. Eng. 1992.

[6] Slocum AH, Braunstein D. Kinematic coupling for thin plates and sheets and the like. U.S. Patent No. 5,915,768 (1999).

[7] Willoughby PJ. Kinematic alignment of precision robotic elements in factory environments. S.M. thesis, Department of Mechanical Engineering, Massachusetts Institute of Technology; 2002.

[8] Hale LC, Slocum AH. Optimal design techniques for kinematic couplings. Prec Eng 2000;25:114–27.

[9] Schouten CH, Rosielle JN, Schellekens PH. Design of a kinematic coupling for precision applications. Prec Eng 1997;20:46–52.

[10] Schmiechen P, Slocum AH. Analysis of kinematic systems: a generalized approach. Prec Eng 1996;19:11–8.

[11] Slocum AH. Design of three-groove kinematic couplings. Prec Eng 1992;14:67–76.

[12] ABB IRB6400R Product Manual. Vasteras, Sweden: ABB Robotics.

[13] Leica LTD500 Product Specifications. http://www.leica-geosystems.com/ims/product/ltd500.htm.

[14] Culpepper ML. Design and application of quasi-kinematic couplings. Ph.D. thesis, Department of Mechanical Engineering, Massachusetts Institute of Technology; 2000.